Electronic Supplementary Information (ESI)

Fast Colloidal Synthesis of Scalable Mo-Rich Hierarchical Ultrathin $MoSe_{2-x}$ Nanosheets for High-Performance Hydrogen Evolution

Xiaoli Zhou,[abc] Jun Jiang,[abc] Tao Ding,[abcd] Jiajia Zhang,[ade] Bicai Pan,[ae] Jian Zuo[a] and Qing Yang*[abcd]

[a] Hefei National Laboratory of Physical Sciences at the Microscale, University of Science and Technology of China (USTC), Hefei 230026, Anhui, P. R. China. E-mail: qyoung@ustc.edu.cn

[b] Department of Chemistry, USTC, Hefei 230026, Anhui, P. R. China.

[c] Laboratory of Nanomaterials for Energy Conversion, USTC, Hefei 230026, Anhui, P. R. China.

[d] Synergetic Innovation Center of Quantum Information & Quantum Physics, USTC, Hefei 230026, Anhui, P. R. China.

[e] Department of Physics, USTC, Hefei 230026, Anhui, P. R. China.

Contents

1. Experimental Section.

Materials. Molybdenum(VI) dioxide bis(acetylacetonate) [$MoO_2(acac)_2$)], tin (II) acetate and oleylamine (OAm, 70%) were purchased from Sigma Aldrich. Dibenzyl diselenide (DBDS, 95%), $W(CO)_6$, tetraphenyl lead (Ph_4Pb) and bulk $MoSe_2$ powder were purchased from Alfa Aesar. The solvents of hexane, ethanol and toluene were all obtained from Shanghai Chemical Reagent Company. All reagents were used as received without further purification.

Characterization. The products were characterized using X-ray powder diffraction (XRD, performed on a Philips X'pert PRO X-ray diffractometer, Cu Kα, λ = 1.54182 Å), scanning electron microscope (SEM, JSM-6700F). The high resolution TEM (HRTEM), high-angle annular dark-field scanning transmission electron microscopy (HAADF-STEM) and corresponding energy-dispersive spectroscopic (EDS) mapping analyses were performed on a JEOL JEM-ARF200F TEM/STEM with a spherical aberration corrector. Raman spectra were performed on a LABRAM-HR spectrometer with a 514.5 nm Ar laser. X-ray photoelectron spectra (XPS) were acquired on an ESCALAB MK II with Mg Kα as the excitation source. Elemental analysis (ICP-AES) of Mo and Se were performed by inductively coupled plasma atomic emission spectroscopy at Galbraith Laboratories (Knoxville, TN). The Fourier transform infrared (FT-IR) spectra were measured on a MAGNA-IR750 (Nicolet Instrument Co., USA). Thermogravimetric analysis (TGA) was performed on a SDTQ600 (TA Instruments) TG-DTA Analyzer under the protection of nitrogen. Nitrogen (N_2) adsorption/desorption isotherms were obtained using Micromeritics ASAP-2000 at 77 K.

Synthesis of hierarchical ultrathin $MoSe_{2-x}$ nanosheets. In a typical procedure, 2 mmol dibenzyl diselenide, 2 mmol $MoO_2(acac)_2$ and 20 mL oleylamine were all added into a 100-mL three-neck round-bottom flask at room temperature. The mixed solution was sealed, and then degassed at 110 °C with high pure Ar atmosphere for 30 min to remove the moisture and oxygen under magnetic stirring. Then the mixture was heated up to 240 °Cat the rate of ~ 10 °C /min, and kept at this temperature for 20 min. Finally, the solution was cooled down to room temperature naturally, and black products precipitated at the bottom of the flask were obtained. 5 mL toluene was then added into the crude solution and the products were isolated by centrifugation (8000 rpm for 5 min). To remove the excess surfactant, the samples were repeatedly washed with toluene and n-hexane.

Annealing of hierarchical ultrathin $MoSe_{2-x}$ nanosheets. As-synthesized $MoSe_{2-x}$ nanosheets were transferred to a quartz glass tube. The tube was then placed in a heating furnace and purged with N_2 for 30 min. Under the N_2, furnace was heated to 450 °C at the rate of 5 °C/min and then was kept at 450 °C for 30 min. The resulting $MoSe_{2-x}$ powder was analyzed by XRD, TEM and FT-IR.

Electrochemical measurements. All of the electrochemical measurements were performed in a three-electrode system on an electrochemical workstation (CHI660E). Typically, 4 mg of catalyst and 30 μL of Nafion solution (Sigma Aldrich, 5 wt%) were dispersed in 1 mL water-ethanol solution with volume ratio

of 4:1 by sonicating for 1 h to form a homogeneous ink. Then 5 μL of the catalyst ink (containing 20 μg of catalyst) was loaded onto a glassy carbon electrode of 3 mm in diameter (loading ~0.285 mg/cm^2). Finally, the as-prepared catalyst film was dried at room temperature.

Linear sweep voltammetry with a scan rate of 2 mV s^{-1} was conducted in 0.5 M H_2SO_4 using a Ag/AgCl (in saturated KCl solution) electrode as the reference electrode, a graphite rod as the counter electrode and the glassy carbon electrode as the working electrode, respectively. The reference electrode was calibrated with respect to reversible hydrogen electrode (RHE). Cyclic voltammetry (CV) was conducted between −0.3 and 0.2 V vs RHE at 50 mV s^{-1} to investigate the cycling stability.

2. Synthesis of ultrathin WSe_2 nanosheets, ultrathin SnSe nanosheets, and PbSe nanocrystals with their XRD patterns and TEM images.

Synthesis of ultrathin WSe_2 nanosheets: $W(CO)_6$ (0.1 mmol), DBDS (0.1 mmol), and oleylamine (OAm, 5 mL) were added into a three-neckflask at room temperature. The reaction solution was degassed with high pure Ar for 30 min at 110°C to remove the moisture and oxygen under magnetic stirring. Then the mixture was heated up to 300 °C at the rate of ~ 10 °C/min, and kept at this temperature for 2h. Once the reaction was finished and cooled down to room temperature, the black products precipitated at the bottom of the flask were purified by centrifugation with excess toluene and n-hexane repeatedly. Other metal selenide nanocrystals were synthesized under same reaction conditions with slight modification as follows.

Synthesis of ultrathin SnSe nanosheets: Tin (II) acetate (0.2 mmol), DBDS (0.1 mmol), and oleylamine (OAm, 6 mL) were added into a three-neck flask at room temperature. Then the mixture was heated up to 280 °C. After 10 min, the resulting ultrathin SnSe nanosheets were obtained.

Synthesis of PbSe nanocrystals: Ph_4Pb (0.2 mmol), DBDS (0.1 mmol), and oleylamine (OAm, 6 mL) were added into a three-neck flask at room temperature. Then the mixture was heated up to 240 °C. After 10 min, the resulting PbSe nanocrystals were obtained.

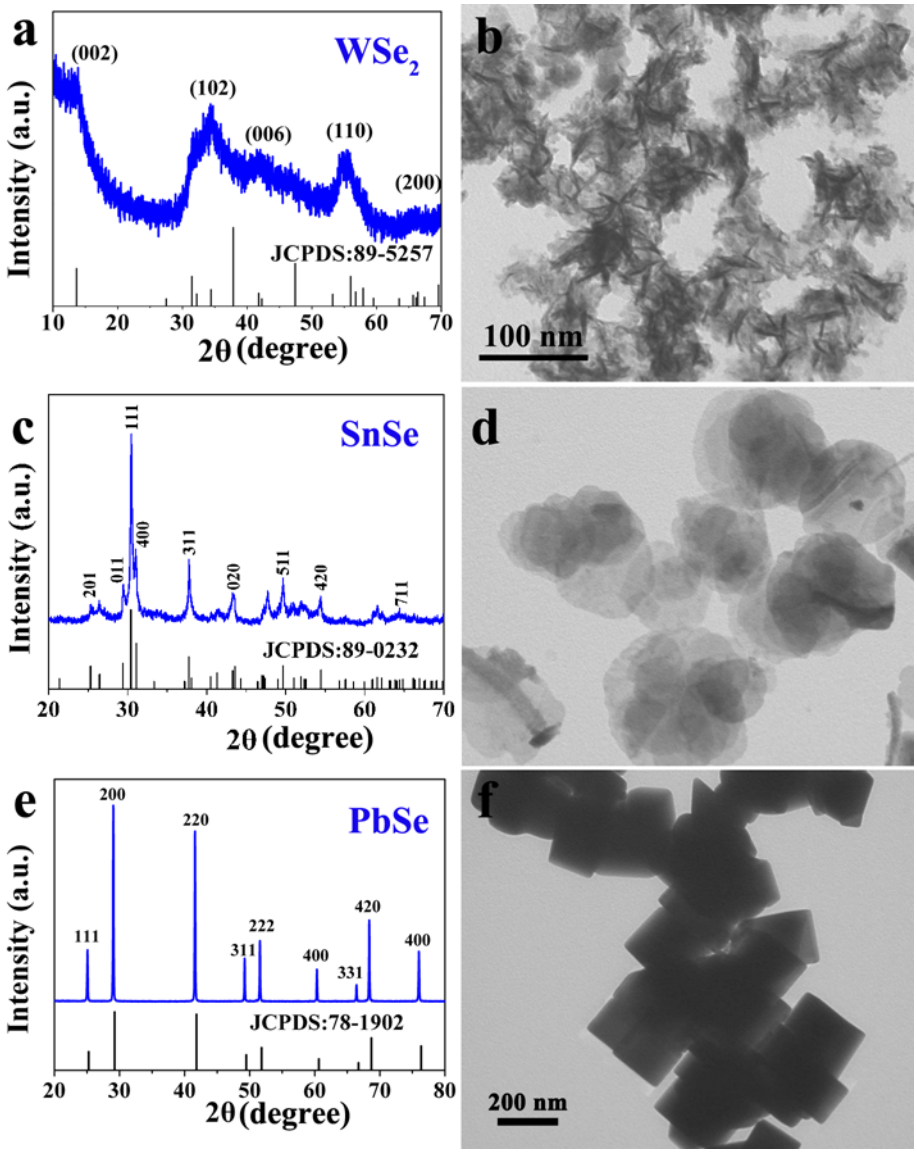

Figure S1. (a) XRD pattern and (b) TEM image of ultrathin WSe_2 nanosheets. (c) XRD pattern and (d) TEM image of ultrathin SnSe nanosheets. (e) XRD pattern and (f) TEM image of PbSe nanocrystals.

3. Photograph of the scalable hierarchical ultrathin $MoSe_{2-x}$ nanosheets.

Figure S2. 0.486 g of the hierarchical ultrathin $MoSe_{2-x}$ nanosheets can be obtained through a one-pot colloidal synthetic route.

4. Photograph of the dispersions of the hierarchical ultrathin $MoSe_{2-x}$ nanosheets in various solvents.

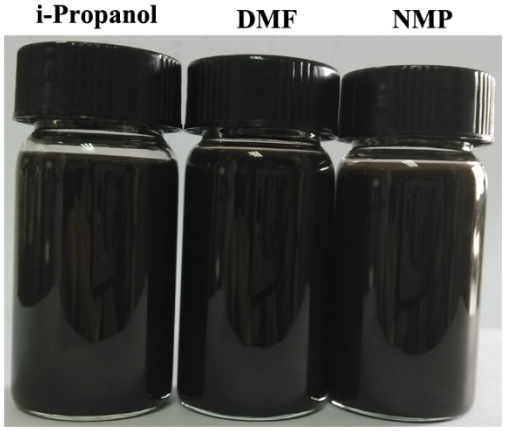

Figure S3. Excellent dispersibility of the hierarchical ultrathin $MoSe_{2-x}$ nanosheets in various solvents. Solvents from left to right: iso-propanol, N,N-dimethyl formamide (DMF) and N-methyl-pyrrolidone (NMP), respectively.

All the dispersions were at a concentration of 2 mg mL^{-1}, and stood still for at least 24 hours before taking photos, suggesting excellent dispersibility which was favorable for practical applications.

5. SEM images of the as-obtained $MoSe_{2-x}$ nanosheets.

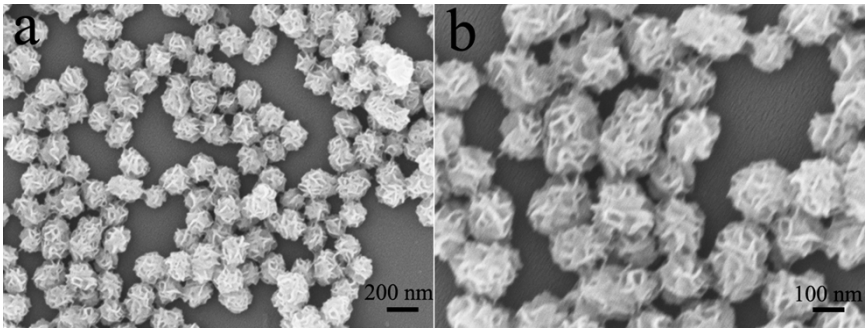

Figure S4. (a) and (b) High-magnified SEM images of the as-obtained $MoSe_{2-x}$ nanosheets.

6. Ultrathin $MoSe_{2-x}$ nanosheets with different Se-Mo-Se atomic layers.

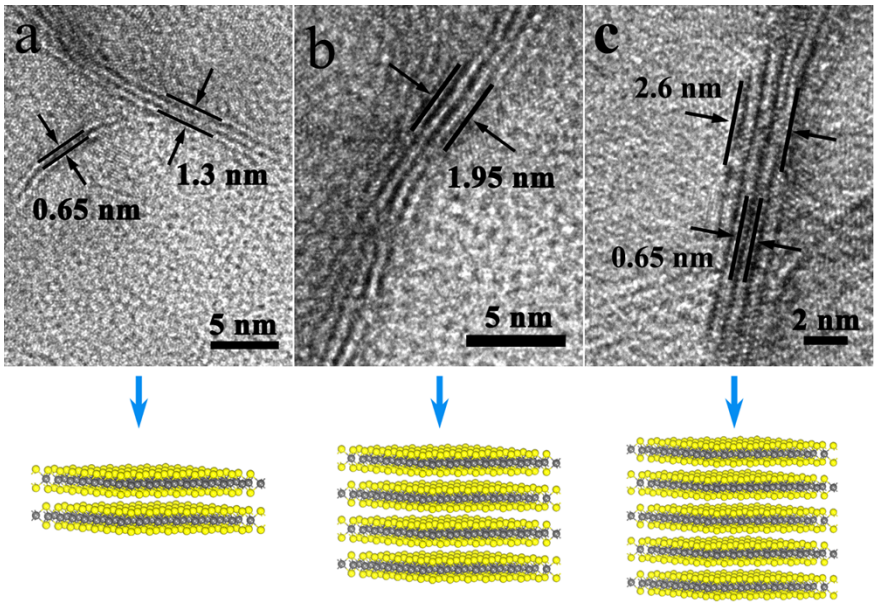

Figure S5. High-resolution TEM images of the folded edge of the synthetic lamellar stacking nanosheets with different Se-Mo-Se atomic layers and the corresponding atomic stacking models. Thicknesses of the curled edges are measured to be 0.65 nm, 1.3 nm, 1.95 nm and 2.6 nm, respectively.

7. Raman spectrum of the as-obtained hierarchical ultrathin $MoSe_{2-x}$ nanosheets.

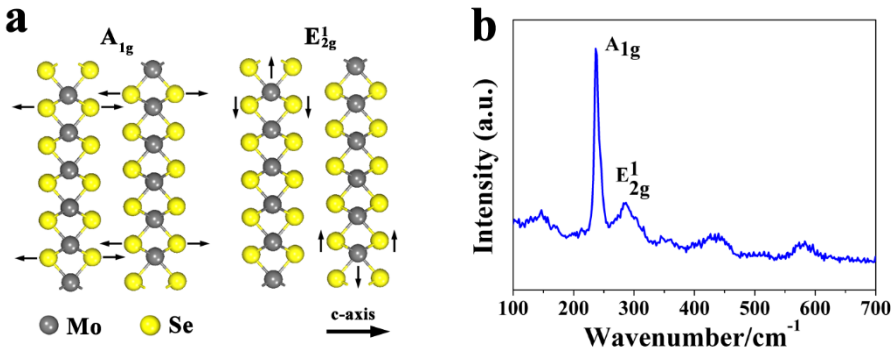

Figure S6. (a) The atomic vibration manners of the A_{1g} and E^1_{2g} vibrational modes of $MoSe_2$. Grey and yellow balls represent Mo and Se atoms, respectively. (b) Raman spectrum showing the characteristic A_{1g} and E^1_{2g} vibrational modes of hierarchical ultrathin $MoSe_{2-x}$ nanosheets, confirming the $MoSe_2$ structure.

8. EDS spectrum of the hierarchical ultrathin $MoSe_{2-x}$ nanosheets.

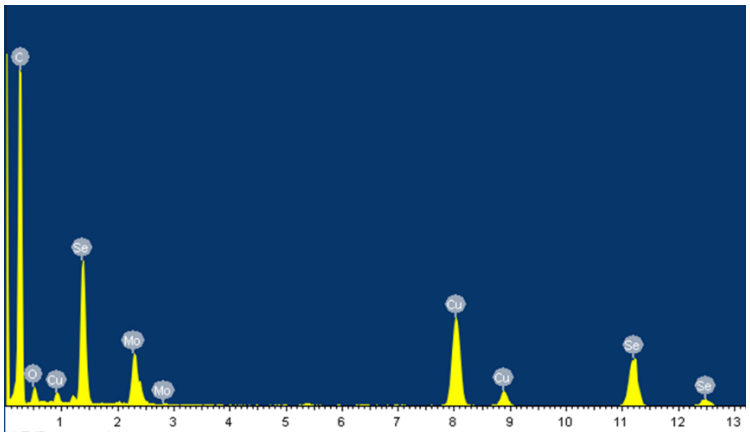

Figure S7. (A) EDS spectrum of the hierarchical ultrathin $MoSe_{2-x}$ nanosheets. The signal of Cu and C arises from the TEM grid made of Cu.

Table 1. Elemental Analyses of the hierarchical ultrathin $MoSe_{2-x}$ nanosheets.

Analysis	**Atomic percentage (%)**		**atomic ratio of Mo/Se**
	Mo	Se	
XPS	11.22	17.18	1:1.53
EDS	39.43	60.57	1:1.53
ICP	34.10	53.80	1:1.58

9. The characterizations of the hierarchical ultrathin $MoSe_{2-x}$ nanosheets before and after annealing for removal of oleylamine.

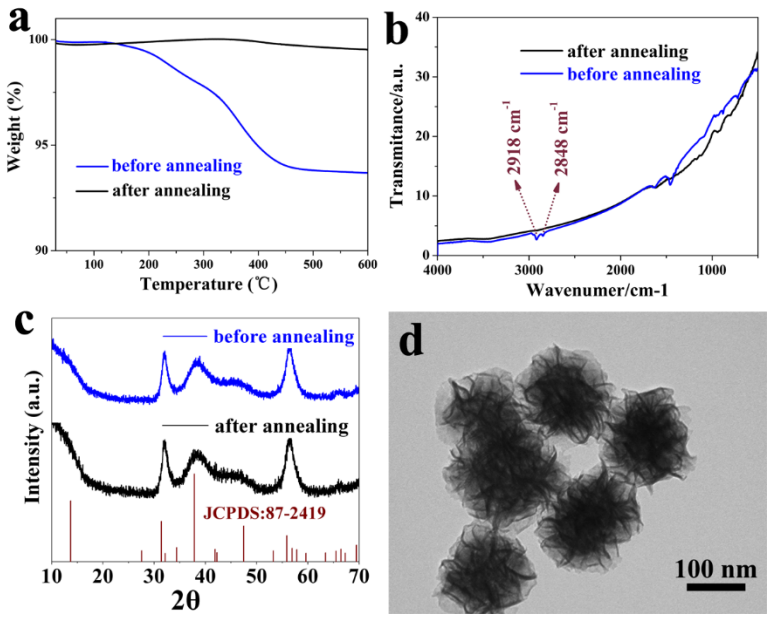

Figure S8. (a) TGA profile of the hierarchical ultrathin $MoSe_{2-x}$ nanosheets heated in N_2 from room temperature up to 900 °C. TGA analysis shows weight loss above 180 °C and leveling off below 500 °C (before annealing: blue curve; after annealing: black curve). (b) Fourier transform infrared (FTIR) spectra of the hierarchical ultrathin $MoSe_{2-x}$ nanosheets before and after annealing. The peaks at 2918 and 2848 cm^{-1} correspond to C-H stretches of oleylamine in the as-prepared sample. (c) XRD patterns of the hierarchical ultrathin $MoSe_{2-x}$ nanosheets before and after annealing. (d) TEM image of the hierarchical ultrathin $MoSe_{2-x}$ nanosheets after annealing.

10. SEM images and XRD pattern of the bulk $MoSe_2$.

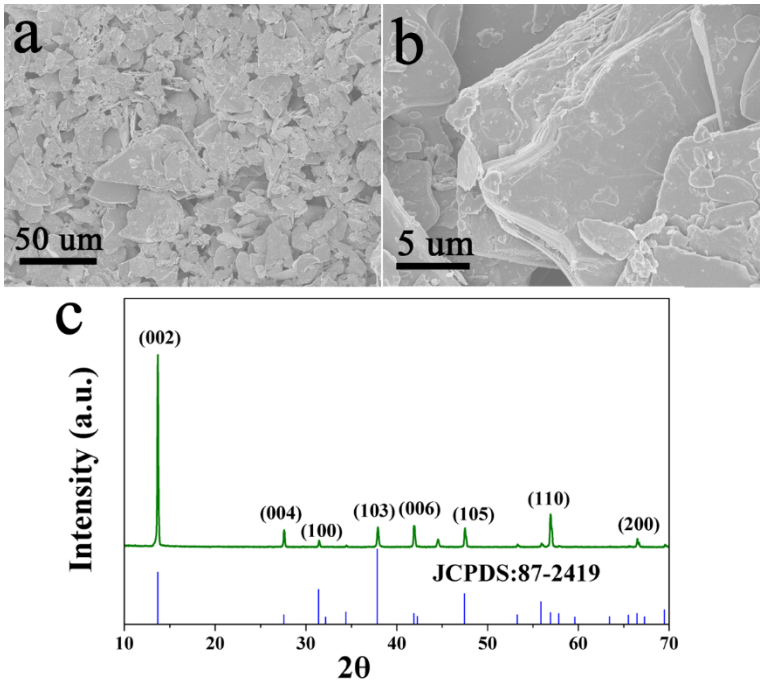

Figure S9. (a-b) SEM images of the bulk $MoSe_2$ with varied magnification, and (c) the corresponding XRD pattern of the bulk $MoSe_2$.

11. Table S2. Comparison of the HER performance for the present hierarchical $MoSe_{2-x}$ nanosheets and other $MoSe_2$-based HER electrocatalysts.

Catalyst	Onset η (mV)	Tafel slope (mV/dec)	η at the j=10 mA/cm^2 (mV)	Ref.
$MoSe_2$ films with Vertically Aligned Layers	200	105−120	-	Nano Lett., 2013, 13, 1341-1347
$MoSe_2$/carbon fiber paper	-	59.8	250	Nano Lett., 2013, 13, 3426-3433
Pure $MoSe_2$ nanosheets	150	101	290	J. Mater. Chem. A, 2014, 2, 360-364
$MoSe_2$/RGO hybrid	50	69	115	
$MoSe_2$ nanosheets	150-260	106	-	J. Mater. Chem. A, 2014, 2, 5597-5601
S-doped $MoSe_2$	90	60	-	
hierarchical $MoSe_{2-x}$ nanosheets	170	98	288	Present work

12. Nitrogen adsorption-desorption isotherms of the hierarchical ultrathin $MoSe_{2-x}$ nanosheets.

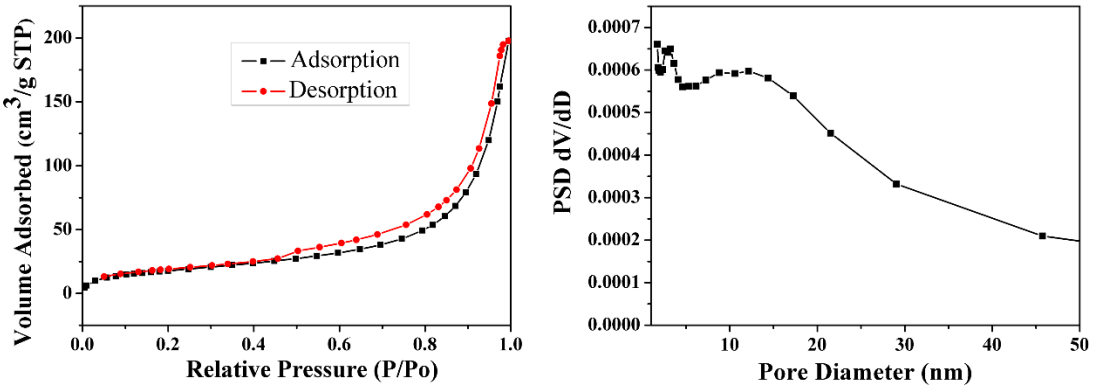

Figure S10. Nitrogen sorption isothermals and the corresponding pore size distribution curve of the hierarchical ultrathin $MoSe_{2-x}$ nanosheets. The specific surface area, mean pore size, and pore volume derived from the adsorption branch are 66.5 m^2/g, 15.8 nm, and 0.3 cm^3/g, respectively.

13. The calculated density of states for the bulk and the monolayer $MoSe_2$ structures

Both the bulk and the monolayer of $MoSe_2$ were treated through using the first-principles calculations. In our calculations, the projected augmented plane wave with the Perdew-Burke-Ernzerhof (PBE) functional encoded in the Vienna ab initio simulation package was employed. For the $MoSe_2$ sheet, we apply periodic boundary conditions with a vacuum region of 20 Å to avoid interactions between the nearest-neighboring sheets. The energy cut-off was set to 500 eV, and the Brillouin zones of the bulk and the $MoSe_2$ sheet were respectively sampled in 12×12×3 and 12×12×1 grids. For the electronic self-consistency loop a total energy convergence criterion of 1×10^{-5} eV was required. Lattice constants and internal coordinates were fully optimized until residual Hellmann–Feynman forces were smaller than 0.01 eV $Å^{-1}$. Figure S11 displays our calculated density of states for the bulk and the nanosheet of $MoSe_2$, where the Fermi level is at 0.0 eV.

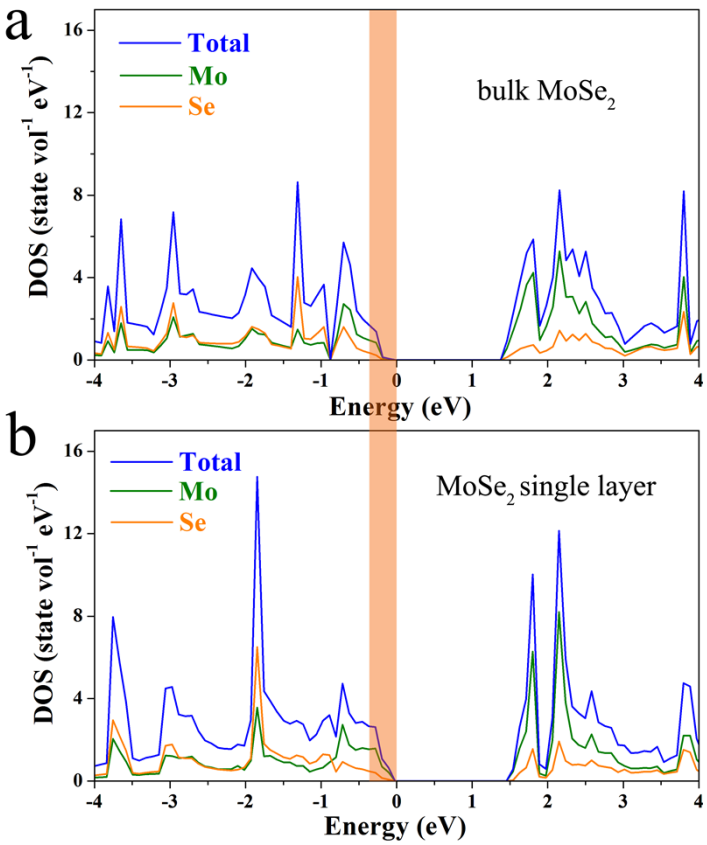

Figure S11. The calculated density of states (DOS) of the single-layered $MoSe_2$ nanosheet and the bulk $MoSe_2$. The shadow part clearly indicates the increase of DOS at the valence band edge of the $MoSe_2$ nanosheet.

14. Electrical property of the hierarchical ultrathin $MoSe_{2-x}$ nanosheets and the bulk $MoSe_2$.

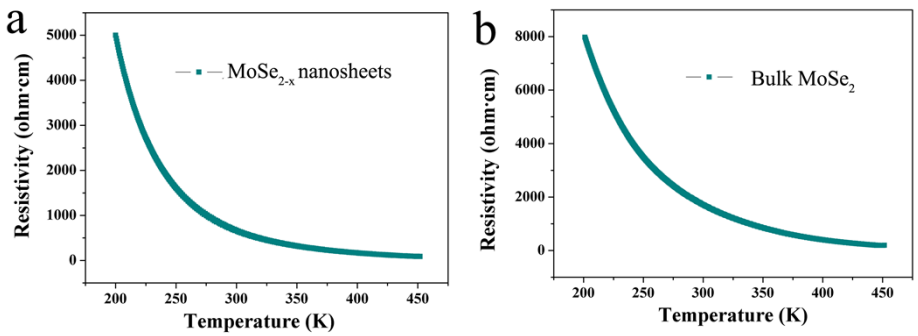

Figure S12. (a) Temperature dependent electrical resistivity of the hierarchical $MoSe_{2-x}$ nanosheets. (b) Temperature dependent electrical resistivity of bulk $MoSe_2$.

The electrical behaviors of the established hierarchical $MoSe_{2-x}$ nanosheets and the bulk $MoSe_2$ have been investigated by the temperature-dependent electrical resistivity. In our case, electrical measurements were performed on pressed pellets of hierarchical $MoSe_{2-x}$ nanosheets and bulk $MoSe_2$. The copper wires

were connected to the samples with silver paste. The measurements were carried out using a Keithley 4200-SCS Semiconductor characterization system by a two probe configuration. Figure S12a and S12b show the typical curves of the temperature-dependent electrical resistivity for $MoSe_{2-x}$ nanosheets and bulk $MoSe_2$, respectively. From the curves, we can clearly observed that the electrical resistivity of the two samples decreased with temperature ranging from 200K to 450K, behaving typical semiconducting characteristic. Of note, the electrical resistivity of the hierarchical $MoSe_{2-x}$ nanosheets at room temperature was about 642.60 Ω·cm while that of the bulk $MoSe_2$ was about 1709.59 Ω·cm. The lower electrical resistivity of the as-obtained $MoSe_{2-x}$ nanosheets would facilitate the rapid charge transport during the reaction, thus promote the catalytic performance for HER.